
LFPO: Likelihood-Free Policy Optimization for Masked Diffusion Models

Chenxing Wei^{*12} Jiazhen Kang³ Hong Wang⁴ Jianqing Zhang⁵ Hao Jiang⁴ Xiaolong Xu⁶ Ningyuan Sun⁶
 Ying He¹ F. Richard Yu⁷ Yao Shu⁸ Bo Jiang⁶

Abstract

Reinforcement Learning with Verifiable Rewards (RLVR) has achieved remarkable success in improving autoregressive models, especially in domains requiring correctness like mathematical reasoning and code generation. However, directly applying such paradigms to Diffusion Large Language Models (dLLMs) is fundamentally hindered by the intractability of exact likelihood computation, which forces existing methods to rely on high-variance approximations. To bridge this gap, we propose Likelihood-Free Policy Optimization (LFPO), a native framework that maps the concept of vector field flow matching to the discrete token space. Specifically, LFPO formulates alignment as geometric velocity rectification, which directly optimizes denoising logits via contrastive updates. This design effectively bypasses the errors inherent in likelihood approximation, yielding the precise gradient estimation. Furthermore, LFPO enforces consistency by predicting final solutions from intermediate steps, effectively straightening the probability flow to enable high-quality generation with significantly fewer iterations. Extensive experiments demonstrate that LFPO not only outperforms state-of-the-art baselines on code and reasoning benchmarks but also accelerates inference by approximately 20% through reduced diffusion steps.

1. Introduction

While *autoregressive* (AR) models have long dominated the landscape of mathematical reasoning and code gener-

ation (Hui et al., 2024; Google, 2025; Anthropic, 2025), recent years have witnessed a paradigm shift as researchers increasingly explore *Diffusion Large Language Models* (dLLMs) (Ye et al., 2025b; Nie et al., 2025) as a compelling alternative (Gong et al., 2025). Fundamentally diverging from the sequential, left-to-right token generation of traditional AR architectures (Tian et al., 2024), dLLMs operate through a holistic denoising mechanism (Li et al., 2025). This unique non-autoregressive nature empowers dLLMs with superior capabilities for global planning (Ye et al., 2025a) and iterative refinement by allowing simultaneous updates (Havasi et al., 2025) to the entire code structure (Zhang et al., 2023), while also enabling significantly faster inference speeds through parallel decoding strategies (Wu et al., 2025; Wang et al., 2025b). Despite these promising capabilities, effectively aligning dLLMs with human intent or correctness feedback remains an open challenge (Zhao et al., 2025; Zhan, 2025).

To address such alignment challenges, *Reinforcement Learning with Verifiable Rewards* (RLVR) (Shao et al., 2024) has established itself as the gold standard for refining AR models in reasoning-heavy domains (Wei et al., 2025; Zhang et al., 2026). Consequently, most existing strategies attempt to transpose these paradigms directly onto dLLMs (Zhao et al., 2025; Zhan, 2025) by forcing the non-Markovian diffusion process into a standard *Markov Decision Process* (MDP) framework (Yang et al., 2025; Wang et al., 2025c) to leverage *Policy Gradient* (PG) (Schulman et al., 2017b). However, a principal challenge inherent in these methods is the computationally intractable log-likelihood of dLLMs (Wang et al., 2025a; Zhao et al., 2025). This limitation is critical because standard policy gradient estimation fundamentally relies on the exact model likelihood (Schulman et al., 2017a) to derive importance sampling weights (Zheng et al., 2025a). Since the exact likelihood is unavailable in diffusion models, these methods are compelled to use ODE/SDE (Chen et al., 2023; Song et al., 2021) discretization to approximate sequence probabilities step-by-step (Gong et al., 2025). In the high-dimensional, discrete token space of dLLMs, such approximations inevitably introduce severe accumulation errors (Zhao et al., 2025) and high computational overhead (Wang et al., 2025c), often resulting in training instability and sub-optimal efficiency (Ni et al., 2025).

^{*}Work done during an internship at Bytedance. ¹Shenzhen University ²Guangdong Laboratory of Artificial Intelligence and Digital Economy (SZ) ³Southeast University ⁴University of Science and Technology of China ⁵Shanghai Jiao Tong University ⁶Bytedance ⁷Carleton University ⁸Hong Kong University of Science and Technology (Guangzhou). Correspondence to: Yao Shu <yaoshu@hkust-gz.edu.cn>, Bo Jiang <jiangbo.jacob@bytedance.com>.

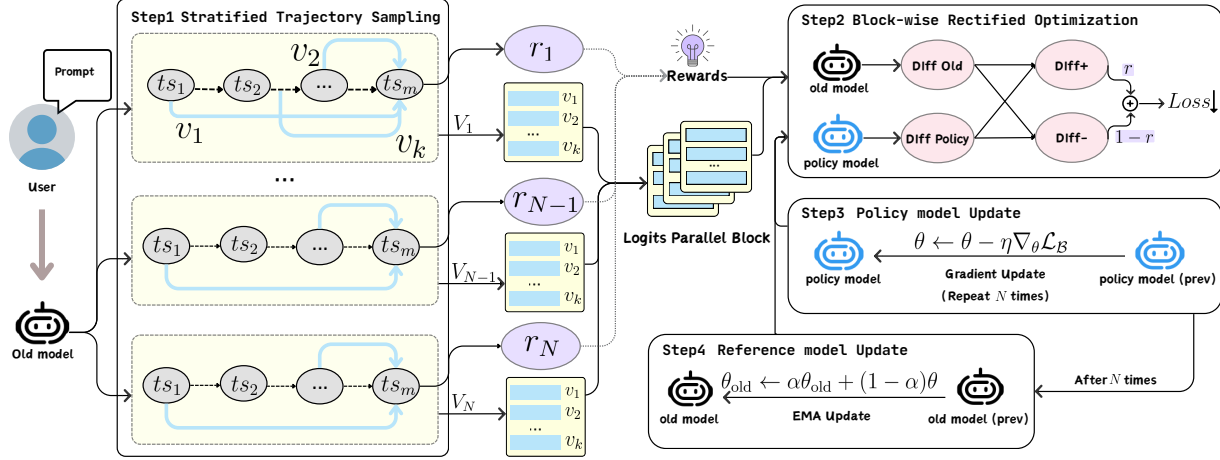


Figure 1. Overview of the LFPO framework. The training pipeline consists of four distinct phases: **Step 1 Generate & Estimate Rewards:** The reference policy π_{old} generates trajectories, and representative timesteps are selected via *Stratified Trajectory Sampling* to reduce variance. **Step 2 Block-wise Rectified Optimization:** Data is partitioned into memory-efficient blocks to enable parallel logit computation. **Step 3 Policy model Update:** The policy π_{θ} is optimized to minimize the deviation from reward-induced implicit policies (π^{+} and π^{-}), effectively performing vector field rectification. **Step 4 Reference model Update:** The reference model is stably updated via *Exponential Moving Average (EMA)*.

We argue that forcing likelihood estimation upon dLLMs is fundamentally intractable (Li et al., 2024) because diffusion models operate through a holistic denoising process where exact likelihoods are mathematically inaccessible (Zhu et al., 2025). This stands in sharp contrast to autoregressive models, whose sequential inference naturally aligns with the MDP paradigm to facilitate straightforward likelihood computation (Xiong et al., 2025). Consequently, existing methods are compelled to rely on costly and often inaccurate estimation approximations.

To address this dilemma, we analyze the generative dynamics of dLLMs through the lens of continuous flow. Drawing inspiration from *Flow Matching (FM)* (Lipman et al., 2023)—which optimizes a vector field to guide distributional transport—we identify a critical theoretical isomorphism in the discrete domain: the predicted logits for masked tokens serve as the discrete projection of the continuous velocity field v (Lou et al., 2024). Leveraging this insight, we propose a fundamental shift in perspective: instead of struggling to approximate the intractable integral $P_{\theta}(x)$, we posit that alignment should be viewed as rectifying these discrete logits (velocity) directly towards high-reward trajectories. By operating in the logit space rather than the probability space, we can bypass the intractable integral entirely and perform efficient policy optimization, resonating with recent theoretical advancements in visual diffusion reinforcement learning that advocate for forward process optimization (Tuo et al., 2025; Zheng et al., 2025b).

To realize this vision, we propose **Likelihood-Free Policy Optimization (LFPO)**, which establishes a new paradigm

for aligning masked diffusion models without reliance on density approximation. The core mechanism of LFPO, illustrated in Figure 1, bypasses the likelihood bottleneck by operating directly in the logit space. Through a contrastive objective, the model learns to rectify its denoising direction, effectively pulling predictions closer to positive outcomes while repelling them from negative ones. By eschewing the noisy approximations inherent in likelihood estimation, LFPO significantly minimizes the variance of error at each update step. This precision ensures a smoother optimization landscape, allowing the model to converge to a performance optimum that is mathematically inaccessible to likelihood-constrained methods. Furthermore, we address the inherent instability of generative trajectories. While traditional diffusion models rely on the precarious smoothness of step-wise denoising—where intermediate noise can easily accumulate and derail the trajectory—LFPO incorporates a robust consistency training objective. This mechanism explicitly trains the model to map arbitrary intermediate states directly to the final solution. Functionally, this imposes a “terminal anchor” on the generative process, forcing all intermediate optimization steps to point towards a unified endpoint. By anchoring the optimization target, LFPO fundamentally suppresses trajectory fluctuations caused by intermediate noise, thereby guaranteeing superior generation stability. Experiments verify the effectiveness of this design: LFPO achieves a 10% average accuracy improvement across reasoning and coding tasks, while simultaneously reducing inference latency by roughly 20% without generation quality degradation. Our contributions are summarized as follows:

- We establish a theoretical isomorphism between continuous FM and discrete Masked Diffusion Models. By identifying denoising logits as the discrete projection of the velocity field, we provide a rigorous justification for rectifying generation trajectories without relying on likelihood-based policy gradients. (Section 3)
- We propose Likelihood-Free Policy Optimization (LFPO), a native RL framework that circumvents intractable likelihood estimation by directly optimizing denoising logits via contrastive regression. This formulation bypasses complex ODE backtracking and enables stable, efficient off-policy training for Masked Diffusion Models. (Section 4)
- We achieve state-of-the-art performance on both mathematical reasoning and code generation benchmarks while significantly accelerating inference. LFPO outperforms likelihood-based baselines and enables high-quality generation with fewer iterative steps through consistency-aware training. (Section 5)

2. Related Work

Diffusion Large Language Models. Discrete denoising diffusion probabilistic models (D3PMs) (Austin et al., 2021a) have recently emerged as a compelling non-autoregressive paradigm for text generation (Yu et al., 2025). Unlike traditional autoregressive models that generate tokens strictly left-to-right, dLLMs generate text via parallel iterative unmasking, offering flexible bidirectional context modeling and potential improvements in decoding efficiency (Ye et al., 2025b). Recent large-scale implementations, such as LLaDA (Nie et al., 2025) and Diffu-Coder (Gong et al., 2025), have demonstrated that dLLMs can achieve language modeling performance competitive with their autoregressive counterparts (Fan et al., 2026). However, while pre-training endows these models with strong general capabilities, effective alignment techniques to enhance their performance remain underexplored.

Reinforcement Learning for Diffusion Alignment. To bridge this gap, recent research has focused on adapting PG methods to the discrete diffusion setting. A prominent line of work utilizes the *Group Relative Policy Optimization* (GRPO) (Shao et al., 2024) framework to enable critic-free optimization. Diffu-GRPO (Zhao et al., 2025) pioneered this direction, introducing the first PG algorithm tailored for masked dLLMs to improve mathematical reasoning. Uni-GRPO (Yang et al., 2025) extended this framework to multimodal domains, unifying reasoning and generation tasks with diversified reward modeling. To address the gradient bias caused by the intractable likelihood of diffusion trajectories, *Sandwiched Policy Gradient* (SPG) (Wang et al., 2025a) proposed leveraging both upper and lower likelihood

bounds. More recently, Coupled-GRPO (Gong et al., 2025) and AGRPO (Zhan, 2025) have been proposed to further improve stability and sample efficiency. Specifically, AGRPO achieves state-of-the-art results by employing Monte Carlo sampling for unbiased policy gradient estimation.

Despite these advancements, the aforementioned methods predominantly remain within the paradigm of maximizing the likelihood (or its surrogates) of high-reward trajectories. We argue that strictly adhering to this likelihood-based objective creates a bottleneck for dLLMs. Rather than persisting with likelihood maximization, we posit that dLLMs require a native RL formulation grounded in their geometric nature. In the continuous domain, FM (Lipman et al., 2023; Liu et al., 2023b) has successfully replaced likelihood objectives with stable vector field regression. While translating this to the discrete domain is non-trivial, recent theoretical works (Zheng et al., 2025b; Liu et al., 2025) have begun to uncover the geometric structures of discrete diffusion. Building on these insights, our work establishes a gradient isomorphism between RL objectives and discrete velocity fields. This perspective motivates us to reframe alignment not as probability maximization, but as velocity rectification, leading to the stable and memory-efficient optimization strategy that we formally derive in the following section.

3. Motivation: A Flow Matching Perspective

Standard reinforcement learning approaches for diffusion models are hindered by the intractability of likelihood computation. To overcome this, we reframe the alignment problem through the lens of FM (Lipman et al., 2023; Liu et al., 2023b). In this section, we first review the continuous framework (Section 3.1), then establish its isomorphism in the discrete domain (Section 3.2), and finally demonstrate that standard dLLM training is theoretically equivalent to optimizing a vector field (Section 3.3).

3.1. Flow Matching

FM (Lipman et al., 2023; Liu et al., 2023b) provides a simulation-free paradigm for training *Continuous Normalizing Flows* (CNFs) (Onken et al., 2021). Consider a probability path $p_t(\mathbf{x})$ defined by a time-dependent vector field $v_t(\mathbf{x})$, which pushes a simple prior distribution p_0 (e.g., Gaussian) to a complex data distribution p_1 via the *Ordinary Differential Equation* (ODE):

$$\frac{d\mathbf{x}}{dt} = v_t(\mathbf{x}), \quad \mathbf{x}(0) \sim p_0. \quad (1)$$

The goal of FM is to regress a neural vector field $v_\theta(\mathbf{x}, t)$ to match a target conditional vector field $u_t(\mathbf{x}|\mathbf{x}_1)$ that generates the desired path from prior to data sample \mathbf{x}_1 . A standard choice is the *Conditional Optimal Transport* path, which interpolates linearly: $\mathbf{x}_t = (1 - t)\mathbf{x}_0 + t\mathbf{x}_1$. The

target velocity is thus constant:

$$u_t(\mathbf{x}_t|\mathbf{x}_1) = \frac{d\mathbf{x}_t}{dt} = \mathbf{x}_1 - \mathbf{x}_0. \quad (2)$$

The objective function minimizes the expected *Mean Squared Error* (MSE) between the model and target velocities:

$$\mathcal{L}_{FM}(\theta) = \mathbb{E}_{t, \mathbf{x}_1, \mathbf{x}_0} [\|v_\theta(\mathbf{x}_t, t) - (\mathbf{x}_1 - \mathbf{x}_0)\|^2]. \quad (3)$$

3.2. Lifting Discrete Tokens to the Probability Simplex

To bridge the gap between continuous Flow Matching and discrete LLMs, we lift the discrete tokens into a continuous geometric space by considering the vocabulary \mathcal{V} as vertices on a probability simplex $\Delta^{V-1} \subset \mathbb{R}^V$, as illustrated in Figure 2. In this geometric formulation, specific data tokens (e.g., Token A, B, C) are represented as deterministic one-hot vectors $\mathbf{x}_1 \in \{0, 1\}^V$ at the vertices, while the [MASK] token is represented as a fixed prior $\mathbf{m} \in \Delta^{V-1}$ located at the center of the simplex (typically the uniform distribution). Within this space, the forward diffusion process—where a token transitions from a masked state to a revealed state—is modeled as a linear interpolation trajectory connecting the mask \mathbf{m} to the target \mathbf{x}_1 : $\mathbf{x}_t = (1 - \alpha_t)\mathbf{m} + \alpha_t\mathbf{x}_1$, where $\alpha_t \in [0, 1]$ represents the noise schedule. Consequently, the **target velocity field** corresponds to the ideal vector difference pointing directly from the mask to the data (shown as the black arrow in Figure 2), given by $u_t = \mathbf{x}_1 - \mathbf{x}_t$.

Crucially, a dLLM parameterized by θ outputs a probability distribution $p_\theta(\cdot|\mathbf{x}_t) = \text{Softmax}(\text{Logits}_t)$ over the vocabulary (depicted as point P_θ inside the simplex). By analogy to the continuous case, we identify the **model velocity field** v_θ as the vector displacement pointing from the mask prior to the current model prediction (green arrow in Figure 2):

$$v_\theta(\mathbf{x}_t, t) := p_\theta(\cdot|\mathbf{x}_t) - \mathbf{x}_t. \quad (4)$$

This identification is pivotal, as it interprets the logits of a dLLM not merely as classification scores, but as the parameterization of the velocity field driving the generative flow.

3.3. Equivalence of Objectives and Methodological Implication

We now demonstrate that training dLLMs with the *Cross-Entropy* (CE) loss is optimization-equivalent to minimizing the FM loss defined above. On the probability simplex Δ^{V-1} , the FM loss simplifies to the Euclidean distance between the model-predicted velocity and the target direction:

$$\mathcal{L}_{FM} = \mathbb{E} [\|(p_\theta - \mathbf{m}) - (\mathbf{x}_1 - \mathbf{m})\|^2] = \mathbb{E} [\|p_\theta - \mathbf{x}_1\|^2]. \quad (5)$$

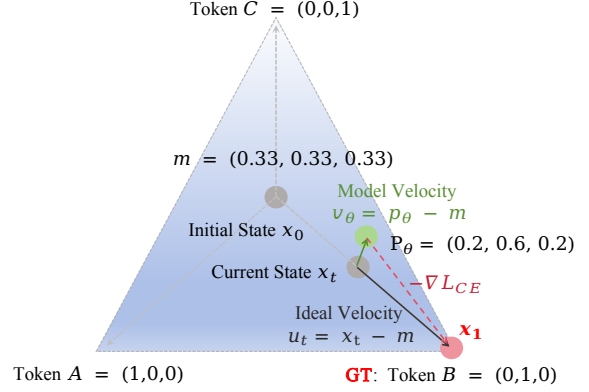


Figure 2. Geometric interpretation of Discrete Lifting (Section 3.2). We visualize the probability simplex Δ^2 for a toy vocabulary of $|\mathcal{V}| = 3$. *Vertices* (Token A, B, C) represent deterministic one-hot data states (e.g., the ground truth target \mathbf{x}_1 corresponds to Token B = [0, 1, 0]). *Interior Points*: (1) \mathbf{m} : The *Mask Prior* (center, [0.33, 0.33, 0.33]), serving as the geometric origin of the flow; (2) \mathbf{x}_t : The *Current State*, modeled as a linear interpolation between the masked state \mathbf{m} and target \mathbf{x}_1 ; (3) P_θ : The *Model Prediction*, a categorical distribution over the vocabulary output by the network. *Vectors (Velocities)*: The *Ideal Velocity* u_t (black arrow) points from the mask towards the true target \mathbf{x}_1 . Crucially, the *Model Velocity* v_θ (green arrow) is defined as the displacement from the mask \mathbf{m} to the prediction P_θ (Eq. 1). The red dashed arrow $-\nabla L_{CE}$ illustrates the optimization direction, rectifying the model velocity towards the ground truth.

The dLLM training minimizes the CE loss:

$$\mathcal{L}_{CE} = \mathbb{E} \left[- \sum_i (\mathbf{x}_1)_i \log(p_\theta)_i \right] = \mathbb{E} [-\log(p_\theta)_k], \quad (6)$$

where k is the index of the ground-truth token. While these objectives reside in different functional spaces (log-likelihood vs. L_2 distance), their optimization dynamics are directionally aligned:

Theorem 3.1 (Gradient Alignment). *Let $\mathbf{z} \in \mathbb{R}^V$ be the pre-softmax logits such that $p_\theta = \text{Softmax}(\mathbf{z})$. For any time step t , the gradient of \mathcal{L}_{CE} with respect to the logits \mathbf{z} is exactly the residual error vector between the model velocity v_θ and the target velocity u_t :*

$$\nabla_{\mathbf{z}} \mathcal{L}_{CE} = p_\theta - \mathbf{x}_1 = v_\theta - u_t. \quad (7)$$

Remark. The detailed proof is provided in Appendix A. Theorem 3.1 formally establishes that standard dLLM training is dynamically optimization-equivalent to minimizing the velocity field error on the probability simplex, as both objectives share the identical gradient direction. We can perform alignment by directly rectifying the velocity field. This motivates our proposed LFPO, which bypasses likelihood estimation entirely by constructing a contrastive objective

that explicitly pulls the logit vector v_θ towards high-reward trajectories and pushes it away from low-reward ones.

4. Policy Alignment via Velocity Rectification

We present LFPO, a reinforcement learning framework tailored for dLLMs. Our method is theoretically grounded in the *Gradient Equivalence* established in Theorem 3.1, which proves that optimizing the CE loss is mathematically equivalent to rectifying the discrete velocity field on the probability simplex.

4.1. Contrastive Velocity Rectification

In the supervised training setting described in Section 3, the optimization target is explicit, as the ground truth data x_0 defines a clear target velocity $u_t = x_0 - m$ that guides the diffusion flow. However, in the RLVR setting, such ground truth is absent. Instead, the model interacts with the environment to sample a trajectory τ and receives only a scalar reward $r(\tau)$ as feedback. The fundamental challenge, therefore, lies in defining a valid supervision target, which corresponds to identifying a correct velocity direction, based solely on this scalar signal.

To address this challenge, we draw inspiration from Theorem 3.2 in Zheng et al. (2025b), which constructs implicit target velocity fields to guide continuous flow matching. We translate this formulation into the discrete logit space. Let π_{ref} denote a frozen reference policy and π_θ denote the current policy. We define the velocity deviation as $\Delta(x_t) = \log \pi_\theta(\cdot|x_t) - \log \pi_{\text{ref}}(\cdot|x_t)$. Based on this, we explicitly define two implicit target policies in the log-space:

$$\log \pi^+(\cdot|x_t) := \log \pi_{\text{ref}}(\cdot|x_t) + \beta \Delta(x_t), \quad (8)$$

$$\log \pi^-(\cdot|x_t) := \log \pi_{\text{ref}}(\cdot|x_t) - \beta \Delta(x_t), \quad (9)$$

where $\beta > 0$ is a scalar hyperparameter. Geometrically, π^+ (*Implicit Positive Policy*) amplifies the deviation of current model from the reference model, while π^- (*Implicit Negative Policy*) reverses this deviation. These definitions provide the gradient targets for the RLVR setting.

Leveraging the reward signal $r(\tau) \in [0, 1]$, we formulate the LFPO objective as a dynamic interpolation between these two implicit targets. We minimize the reward-weighted CE loss between the velocity field of model and these targets:

$$\begin{aligned} \mathcal{L}_{\text{LFPO}}(\theta) = \mathbb{E}_{\tau \sim \pi_\theta} \left[\mathbb{E}_t \left[r(\tau) \cdot \text{CE}(\pi^+, \pi_\theta) \right. \right. \\ \left. \left. + (1 - r(\tau)) \cdot \text{CE}(\pi^-, \pi_\theta) \right] \right], \end{aligned} \quad (10)$$

where $\text{CE}(P, Q) = -\sum P(x) \log Q(x)$. Intuitively, high rewards ($r \rightarrow 1$) drive the policy to align with π^+ (pull), while low rewards ($r \rightarrow 0$) drive it towards π^- (push).

While theoretically sound, directly optimizing Eq. (10) presents practical challenges. Naively sampling a single timestep t results in high gradient variance and optimization instability. To mitigate this, we adopt *Stratified Trajectory Sampling* to ensure dense temporal coverage. However, this multi-sample approach imposes a severe memory burden on the GPU. Consequently, we introduce *Block-wise Gradient Accumulation* to resolve the memory bottleneck, which we detail in the following subsections.

4.2. Scalable and Stable Gradient Estimation

Stratified Trajectory Sampling. The masked diffusion process involves a discrete transition sequence $x_T \rightarrow \dots \rightarrow x_0$. Naive random sampling of a single timestep t yields high-variance gradients due to the non-uniform difficulty of denoising across different stages of generation. To address this, we propose *Stratified Trajectory Sampling* to ensure dense temporal coverage. Specifically, for a trajectory of length L , we partition the valid timestep range into K uniform segments. In each training step, we sample exactly one timestep t_k from each segment:

$$t_k \sim \mathcal{U} \left[\lfloor k \cdot \frac{L}{K} \rfloor, \lfloor (k+1) \cdot \frac{L}{K} \rfloor - 1 \right], \quad (11)$$

$$k = 0, \dots, K - 1.$$

Block-wise Gradient Accumulation. Estimating the accurate velocity direction for rectifying the policy requires aggregating statistics from multiple trajectories. Given a batch size B , we sample N trajectories per prompt, and for each trajectory, we calculate gradients at K stratified timesteps. This results in an explosive computational tensor size of $B \times N \times K$. To resolve this bottleneck, we implement a *Block-wise Gradient Accumulation* scheme. We partition the total $B \times N \times K$ samples into smaller, memory-efficient blocks. The optimization follows a hybrid parallel-serial execution: we compute gradients in parallel within each block to leverage GPU parallelism, and then serially accumulate these gradients across blocks. This technique allows us to scale up the effective batch size by an order of magnitude without hardware upgrades, significantly reducing the variance of the policy gradient.

4.3. LFPO

The complete training procedure of LFPO is summarized in Algorithm 1. In the initial data collection phase (lines 3-6), we sample N diverse trajectories for each prompt using the reference policy π_{old} (line 4). We then evaluate these trajectories to compute scalar rewards r based on the specific downstream task, such as answer correctness for mathematical reasoning or execution pass rate for code generation. These samples and their corresponding rewards are aggregated into a batch dataset $\mathcal{D}_{\text{batch}}$.

Algorithm 1 Likelihood-Free Policy Optimization (LFPO)

```

1: Input: Dataset  $\mathcal{D}$ , Policy  $\pi_\theta$ , Reference  $\pi_{\text{old}}$ , Params
    $\beta, N, K, \eta, \alpha$ .
2: repeat
3:   // Phase 1: Generate & Estimate Rewards
4:   For batch queries  $Q \subset \mathcal{D}$ , sample  $N$  trajectories
      $\mathcal{Y}_q \sim \pi_{\text{old}}(\cdot|q)$ .
5:   Compute rewards  $r_{\mathbf{y}} = \text{reward}(\mathbf{y})$  for all  $\mathbf{y}$ .
6:    $\mathcal{D}_{\text{batch}} \leftarrow \bigcup_{q \in Q} \{(\mathbf{y}, r_{\mathbf{y}}) \mid \mathbf{y} \in \mathcal{Y}_q\}$ .
7:   // Phase 2: Block-wise Rectified Optimization
8:   Partition  $\mathcal{D}_{\text{batch}}$  into blocks  $\{\mathcal{B}_1, \dots, \mathcal{B}_M\}$ .
9:   for each block  $\mathcal{B}_m$  do
10:    Sample stratified timesteps  $\mathcal{T}_{\mathbf{y}} = \{t_1, \dots, t_K\}$  for
      all  $\mathbf{y} \in \mathcal{B}_m$ .
11:    Compute block loss (parallel):

      
$$\mathcal{L}_{\mathcal{B}} = \sum_{(\mathbf{y}, r) \in \mathcal{B}_m} \sum_{t \in \mathcal{T}_{\mathbf{y}}} \left[ r \cdot \text{CE}^+ + (1 - r) \cdot \text{CE}^- \right]$$


12:    Update:  $\theta \leftarrow \theta - \eta \nabla_{\theta} \mathcal{L}_{\mathcal{B}}$ .
13:    Delete computation graph to free VRAM.
14:  end for
15:  // Phase 3: Reference Update
16:   $\theta_{\text{old}} \leftarrow \alpha \theta_{\text{old}} + (1 - \alpha) \theta$ .
17: until convergence
    
```

Subsequently, to optimize the policy under memory constraints, we employ a block-wise rectified optimization strategy (lines 8-15). We partition the dataset into memory-efficient blocks (line 9) and apply Stratified Trajectory Sampling to select K representative timesteps for each trajectory (line 11). We leverage an optimized parallel computation scheme where gradients for all trajectories and timesteps within a block are computed simultaneously (line 12). The model parameters θ are updated immediately after processing each block (line 13), followed by an explicit deletion of the computation graph to prevent VRAM overflow (line 14). Finally, to ensure training stability, the reference model π_{old} is updated via Exponential Moving Average (EMA) at the end of each iteration (line 17):

$$\theta_{\text{old}} \leftarrow \alpha \theta_{\text{old}} + (1 - \alpha) \theta, \quad (12)$$

where α is the decay rate and θ_{old} represents the parameters of π_{old} .

5. Empirical Results

In this section, we provide a comprehensive evaluation of LFPO across code generation and mathematical reasoning domains. Our analysis aims to validate not only the superior performance of the proposed framework but also the efficiency gains inherent to its likelihood-free design. To structure our analysis, we organize the remainder of this

section as follows: Section 5.1 first details the experimental setup, including the baselines, benchmarks, and reward configurations. Subsequently, Section 5.2 presents the main results, dissecting the method’s impact on downstream performance, inference latency, and training convergence speed. Finally, Section 5.3 provides an in-depth ablation study to isolate the geometric contributions of the attraction (positive) and repulsion (negative) terms within our objective.

5.1. Experimental Setup

We evaluate LFPO using DiffuCoder (Gong et al., 2025) (code) and LLaDA 8B (Nie et al., 2025) (reasoning) against state-of-the-art RL baselines, including Diffu/Coupled-GRPO (Zhao et al., 2025; Gong et al., 2025), Uni-GRPO (Yang et al., 2025), SPG (Wang et al., 2025a), and AGRPO (Zhan, 2025).

Benchmarks and Data Strategy. We employ distinct protocols for each domain. For code generation, we target *Out-of-Domain Generalization*: models are trained on AceCode-87K (Zeng et al., 2025) and zero-shot evaluated on HumanEval (Chen et al., 2021), MBPP (Austin et al., 2021b), EvalPlus (Liu et al., 2023a), and BigCodeBench (Zhuo et al., 2025). Conversely, reasoning tasks follow standard *In-Domain Evaluation* using training/test splits of math benchmarks (GSM8K (Cobbe et al., 2021), MATH (Hendrycks et al., 2021)) and general datasets (Hellaswag (Zellers et al., 2019), GPQA (Rein et al., 2024), WinoGrande (Sakaguchi et al., 2019), PIQA (Bisk et al., 2019)).

Implementation Details. Our likelihood-free framework utilizes sparse rewards: syntax compliance and pass rates for code, and format/accuracy for reasoning. We use AdamW with memory-efficient block-wise optimization. Generation is configured with a maximum length of 512 and 2048 diffusion steps, accelerated by confidence-based early stopping to balance efficiency and quality.

5.2. Main Results

Performance Superiority via Accurate Gradient Estimation. We first examine the generation quality on downstream tasks. As reported in Table 1 and Table 2, LFPO consistently outperforms both the base models and likelihood-based RL baselines across all metrics. In the code generation domain, LFPO achieves a remarkable average score of 60.8, surpassing the strong baseline AGRPO (60.6). Specifically, on the foundational HumanEval benchmark, our method achieves a score of 75.6, representing a 3.6% absolute improvement over the base DiffuCoder. The advantage is even more pronounced in the reasoning domain (Table 2), where LFPO establishes a new state-of-the-art. Notably, on the challenging GSM8K and MATH benchmarks, our method yields substantial gains of 9.9% and 7.0%, respectively,

LFPO: Likelihood-Free Policy Optimization for Masked Diffusion Models

Table 1. Main Results on Code Generation Benchmarks. We compare LFPO against the base model DiffuCoder and various reinforcement learning baselines. The values in red parentheses denote the absolute improvement over the base model. LFPO (Pos. Only) and LFPO (Neg. Only) refer to ablation variants optimized solely with the positive loss or the negative loss, respectively, while LFPO (All Loss) utilizes the full contrastive velocity rectification objective. The best results are highlighted in bold, and the second-best results are underlined.

Model	HumanEval	HumanEval+	MBPP	MBPP+	EvalPlus	BigCodeBench Full	BigCodeBench Hard	Avg.
DiffuCoder	72.0	65.2	75.1	61.9	63.6	35.7	12.2	53.7
+ diffu-GRPO	73.1 (+1.1)	66.1 (+0.9)	77.3 (+2.2)	67.3 (+5.4)	67.9 (+4.3)	39.2 (+3.5)	12.5 (+0.3)	57.6 (+3.9)
+ UniGRPO	74.5 (+2.5)	67.2 (+2.0)	78.9 (+3.8)	68.8 (+6.9)	70.3 (+6.7)	42.6 (+6.9)	<u>12.9 (+0.7)</u>	59.3 (+5.6)
+ SPG	74.6 (+2.6)	69.1 (+3.9)	80.2 (+5.1)	69.2 (+7.3)	68.9 (+5.3)	42.1 (+6.4)	<u>12.9 (+0.7)</u>	59.6 (+5.9)
+ coupled-GRPO	73.2 (+1.2)	68.3 (+3.1)	78.6 (+3.5)	67.5 (+5.6)	67.9 (+4.3)	40.4 (+4.7)	10.8 (-1.4)	56.5 (+2.8)
+ AGRPO	<u>75.3 (+3.3)</u>	70.2 (+5.0)	<u>80.3 (+5.2)</u>	71.7 (+9.8)	69.3 (+5.7)	<u>44.6 (+8.9)</u>	13.1 (+0.9)	<u>60.6 (+6.9)</u>
+ LFPO (Pos. Only)	73.2 (+1.2)	67.3 (+2.1)	80.1 (+5.0)	68.2 (+6.3)	68.3 (+4.7)	43.1 (+7.4)	12.4 (+0.2)	58.9 (+5.2)
+ LFPO (Neg. Only)	73.1 (+1.1)	67.2 (+2.0)	79.5 (+4.4)	68.5 (+6.6)	68.9 (+5.3)	43.4 (+7.7)	12.5 (+0.3)	59.0 (+5.3)
+ LFPO (All Loss)	75.6 (+3.6)	<u>70.1 (+4.9)</u>	81.6 (+6.5)	<u>71.3 (+9.4)</u>	<u>69.5 (+5.9)</u>	44.8 (+9.1)	<u>12.9 (+0.7)</u>	60.8 (+7.1)

Table 2. Main Results on Reasoning Benchmarks. We compare LFPO against the base model LLaDA 8B and various reinforcement learning baselines. The values in red parentheses denote the absolute improvement over the base model. LFPO (Pos. Only) and LFPO (Neg. Only) refer to ablation variants optimized solely with the positive attraction term or the negative repulsion term, respectively, while LFPO (All Loss) utilizes the full contrastive velocity rectification objective. The best results are highlighted in bold, and the second-best results are underlined.

Model	GSM8K	MATH	GPQA	Hellaswag	WinoGrande	PIQA	Avg.
LLaDA 8B	69.7	30.6	25.3	70.3	75.8	71.6	57.2
+ diffu-GRPO	74.3 (+4.6)	33.7 (+3.1)	26.1 (+0.8)	80.1 (+9.8)	83.2 (+7.4)	79.3 (+7.7)	62.8 (+5.6)
+ UniGRPO	77.2 (+7.5)	34.5 (+3.9)	26.2 (+0.9)	82.3 (+12.0)	84.7 (+8.9)	81.2 (+9.6)	64.4 (+7.2)
+ SPG	76.2 (+6.5)	34.1 (+3.5)	25.9 (+0.6)	83.1 (+12.8)	84.3 (+8.5)	80.9 (+9.3)	64.1 (+6.9)
+ coupled-GRPO	75.1 (+5.4)	33.9 (+3.3)	25.7 (+0.4)	82.5 (+12.2)	85.6 (+9.8)	83.2 (+11.6)	64.3 (+7.1)
+ AGRPO	<u>78.3 (+8.6)</u>	<u>36.1 (+5.5)</u>	27.3 (+2.0)	<u>85.1 (+14.8)</u>	87.3 (+11.5)	<u>85.6 (+14.0)</u>	<u>66.6 (+9.4)</u>
+ LFPO (Pos. Only)	<u>78.3 (+8.6)</u>	35.2 (+4.6)	26.1 (+0.8)	84.2 (+13.9)	83.1 (+7.3)	80.6 (+9.0)	64.6 (+7.4)
+ LFPO (Neg. Only)	78.1 (+8.4)	34.9 (+4.3)	26.3 (+1.0)	84.3 (+14.0)	83.7 (+7.9)	79.6 (+8.0)	64.5 (+7.3)
+ LFPO (All Loss)	79.6 (+9.9)	37.6 (+7.0)	<u>27.1 (+1.8)</u>	85.7 (+15.4)	<u>86.9 (+11.1)</u>	85.9 (+14.3)	67.1 (+9.9)

over LLaDA 8B. We attribute this superior performance primarily to the fact that LFPO **bypasses the approximation of intractable likelihoods**. Unlike likelihood-based methods (e.g., AGRPO) that rely on surrogate objectives or high-variance importance sampling, LFPO formulates optimization as a direct regression. This results in significantly more accurate gradient estimation with minimal variance, effectively preventing the policy from getting stuck in sub-optimal local minima and enabling the model to converge to a superior optimum.

Inference Efficiency via Optimal Trajectory Learning.

A critical bottleneck for diffusion language models is the high computational cost associated with iterative denoising. Table 3 highlights a key advantage of our approach: LFPO significantly accelerates inference while improving performance. As indicated by the values in red parentheses, our method reduces the average inference steps by approximately 41.8 steps for code tasks and 159.0 steps for rea-

soning tasks compared to the base model. In stark contrast, baselines like AGRPO often degrade efficiency (increasing steps by +73.6 on MATH) to achieve marginal performance gains. This divergence stems from the fundamental difference in optimization objectives. Likelihood maximization tends to overfit to the specific, often meandering trajectories of the training data. Conversely, by treating generation as a flow matching problem, LFPO encourages the model to learn the most direct vector field from the mask prior to the data distribution. This effectively straightens the generation trajectory, allowing the model to reach high-quality solutions with significantly fewer intermediate steps.

Training Convergence via Computational Efficiency.

Beyond inference, we further demonstrate the sample efficiency of our training framework in Figure 3. The curves illustrate that LFPO (red) achieves drastically faster convergence compared to the baseline AGRPO (blue). Quantitatively, our method matches the peak performance of

Table 3. **Unified Efficiency Analysis.** We report the average inference steps per problem across selected code generation and reasoning benchmarks. **Avg.** represents the mean steps within each task category. The values in **red parentheses** denote the reduction in inference steps (efficiency improvement) compared to the Base Model. *Base Model* refers to DiffuCoder for code tasks and LLaDA 8B for reasoning tasks. Lower values (\downarrow) indicate better efficiency.

Model	Code Generation				Reasoning			
	HumanEval	MBPP	BCB-Full	Avg.	GSM8K	MATH	Hellaswag	Avg.
Base Model [†]	253.7	317.2	426.3	332.4	1034.2	1536.3	1036.7	1202.4
+ diffu-GRPO	254.3 (+0.6)	305.4 (-11.8)	430.7 (+4.4)	330.1 (-2.3)	1048.4 (+14.2)	1547.4 (+11.1)	1027.8 (-8.9)	1207.9 (+5.5)
+ UniGRPO	248.0 (-5.7)	319.3 (+2.1)	443.3 (+17.0)	336.9 (+4.5)	1020.3 (-13.9)	1539.3 (+3.0)	985.8 (-50.9)	1181.8 (-20.6)
+ SPG	243.7 (-10.0)	305.8 (-11.4)	416.7 (-9.6)	322.1 (-10.3)	1071.0 (+36.8)	1576.7 (+40.4)	1009.1 (-27.6)	1218.9 (+16.5)
+ coupled-GRPO	262.2 (+8.5)	326.5 (+9.3)	431.2 (+4.9)	340.0 (+7.6)	1015.9 (-18.3)	1601.6 (+65.3)	1025.8 (-10.9)	1214.4 (+12.0)
+ AGRPO	254.2 (+0.5)	313.9 (-3.3)	438.5 (+12.2)	335.5 (+3.1)	1004.8 (-29.4)	1609.9 (+73.6)	1063.6 (+26.9)	1226.1 (+23.7)
+ LFPO (Pos. Only)	223.6 (-30.1)	292.3 (-24.9)	373.4 (-52.9)	296.4 (-36.0)	911.3 (-122.9)	1355.3 (-181.0)	893.1 (-143.6)	1053.2 (-149.2)
+ LFPO (Neg. Only)	234.7 (-19.0)	286.7 (-30.5)	377.3 (-49.0)	299.6 (-32.8)	909.7 (-124.5)	1367.9 (-168.4)	891.2 (-145.5)	1056.3 (-146.1)
+ LFPO (All Loss)	218.3 (-35.4)	282.3 (-34.9)	371.2 (-55.1)	290.6 (-41.8)	891.2 (-143.0)	1348.9 (-187.4)	890.2 (-146.5)	1043.4 (-159.0)

[†] Base Model corresponds to **DiffuCoder** for Code Generation datasets and **LLaDA 8B** for Reasoning datasets.

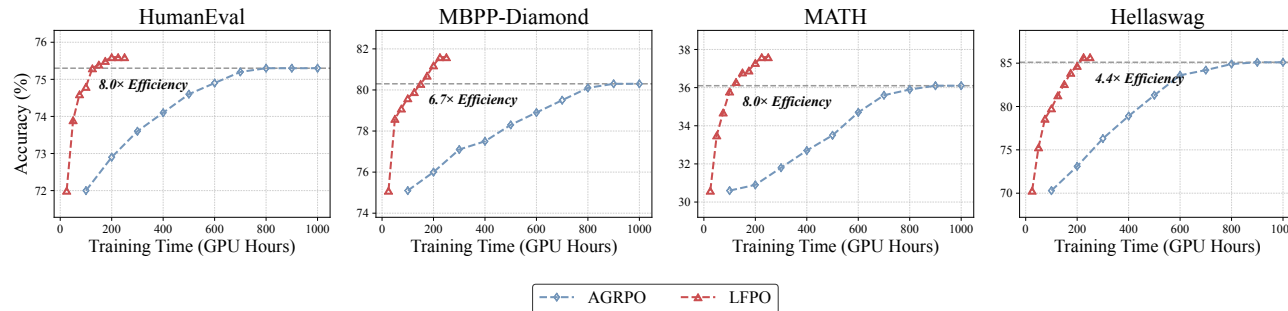


Figure 3. **Convergence Analysis on Code and Reasoning Tasks.** The plots show accuracy progression against training time (GPU Hours). The red curve represents our proposed LFPO, while the blue curve represents the baseline AGRPO. The horizontal dashed line marks the final converged accuracy of the baseline. Notably, LFPO requires substantially less training time to match or surpass the baseline’s best performance, highlighting its superior sample efficiency and convergence speed.

the baseline $8.0\times$ faster on HumanEval and MATH, and $4.4\times$ faster on Hellaswag. We attribute this dramatic acceleration to two synergistic factors inherent to our system design. First and foremost, our Block-wise Rectified Optimization strategy (Section 4.2) fundamentally enhances computational throughput. By partitioning long trajectories into manageable blocks, we enable massively parallel logit computation while maintaining memory efficiency. This allows for high-speed training steps without sacrificing the correctness of the optimization, significantly outperforming the sequential or memory-bound computations in baselines. Second, the training loop benefits from the model’s accelerated generation capability. As LFPO learns to produce high-quality outputs with fewer diffusion steps, the computational cost of the inference phase within each training iteration is drastically reduced. This creates a virtuous cycle where faster data collection leads to more frequent gradient updates per wall-clock hour, resulting in the rapid convergence observed in our experiments.

5.3. Ablation Study

To dissect the geometric mechanisms driving LFPO, we analyze variants optimized with partial objectives: *Pos. Only* (Attraction) and *Neg. Only* (Repulsion). As shown in Tables 1 and 2, both variants yield improvements over the base model, yet neither matches the performance of the full *All Loss* objective. From a geometric perspective on the probability simplex (as illustrated in Figure 1), the *Pos. Only* term acts as an attraction force, pulling the model’s velocity v_θ towards the vertex of the correct token x_1 . The results show this is crucial for reasoning accuracy (e.g., GSM8K). Conversely, the *Neg. Only* term acts as a repulsion force, pushing the velocity away from incorrect vertices. The superior performance of the combined objective confirms that shaping the vector field requires a contrastive approach: simultaneously encouraging correct directions while actively suppressing deviation into low-reward regions ensures the most robust generative flow.

6. Conclusions

We proposed LFPO, which aligns dLLMs to bypass intractable likelihoods, supported by efficient stratified sampling and block-wise optimization. Empirically, LFPO establishes superior performance across code and reasoning benchmarks while significantly accelerating both training convergence and inference generation.

Impact Statement

This paper presents work whose goal is to advance the field of Reinforcement Learning. There are many potential societal consequences of our work, none which we feel must be specifically highlighted here.

References

- Anthropic. Claude code: Best practices for agentic coding. <https://www.anthropic.com/engineering/claude-code-best-practices>, 2025. Accessed: 2025.
- Austin, J., Johnson, D. D., Ho, J., Tarlow, D., and van den Berg, R. Structured denoising diffusion models in discrete state-spaces. In Beygelzimer, A., Dauphin, Y., Liang, P., and Vaughan, J. W. (eds.), *Advances in Neural Information Processing Systems*, 2021a. URL <https://openreview.net/forum?id=h7-XixPCAL>.
- Austin, J., Odena, A., Nye, M., Bosma, M., Michalewski, H., Dohan, D., Jiang, E., Cai, C., Terry, M., Le, Q., and Sutton, C. Program synthesis with large language models, 2021b. URL <https://arxiv.org/abs/2108.07732>.
- Bisk, Y., Zellers, R., Bras, R. L., Gao, J., and Choi, Y. Piqa: Reasoning about physical commonsense in natural language, 2019. URL <https://arxiv.org/abs/1911.11641>.
- Chen, M., Tworek, J., Jun, H., Yuan, Q., de Oliveira Pinto, H. P., Kaplan, J., Edwards, H., Burda, Y., Joseph, N., Brockman, G., Ray, A., Puri, R., Krueger, G., Petrov, M., Khlaaf, H., Sastry, G., Mishkin, P., Chan, B., Gray, S., Ryder, N., Pavlov, M., Power, A., Kaiser, L., Bavarian, M., Winter, C., Tillet, P., Such, F. P., Cummings, D., Plappert, M., Chantzis, F., Barnes, E., Herbert-Voss, A., Guss, W. H., Nichol, A., Paino, A., Tezak, N., Tang, J., Babuschkin, I., Balaji, S., Jain, S., Saunders, W., Hesse, C., Carr, A. N., Leike, J., Achiam, J., Misra, V., Morikawa, E., Radford, A., Knight, M., Brundage, M., Murati, M., Mayer, K., Welinder, P., McGrew, B., Amodei, D., McCandlish, S., Sutskever, I., and Zaremba, W. Evaluating large language models trained on code, 2021. URL <https://arxiv.org/abs/2107.03374>.
- Chen, S., Chewi, S., Lee, H., Li, Y., Lu, J., and Salim, A. The probability flow ODE is provably fast. In *Thirty-seventh Conference on Neural Information Processing Systems*, 2023. URL <https://openreview.net/forum?id=KD6MFeWSAd>.

- Cobbe, K., Kosaraju, V., Bavarian, M., Chen, M., Jun, H., Kaiser, L., Plappert, M., Tworek, J., Hilton, J., Nakano, R., Hesse, C., and Schulman, J. Training verifiers to solve math word problems, 2021. URL <https://arxiv.org/abs/2110.14168>.
- Fan, C., Heng, W., Li, B., Liu, S., Song, Y., Su, J., Qu, X., Shen, K., and Wei, W. Stable-diffcoder: Pushing the frontier of code diffusion large language model, 2026. URL <https://arxiv.org/abs/2601.15892>.
- Gong, S., Zhang, R., Zheng, H., Gu, J., Jaitly, N., Kong, L., and Zhang, Y. Diffucoder: Understanding and improving masked diffusion models for code generation, 2025. URL <https://arxiv.org/abs/2506.20639>.
- Google. Gemini 3. <https://aistudio.google.com/models/gemini-3>, 2025. Accessed: 2025.
- Havasi, M., Karrer, B., Gat, I., and Chen, R. T. Q. Edit flows: Variable length discrete flow matching with sequence-level edit operations. In *The Thirty-ninth Annual Conference on Neural Information Processing Systems*, 2025. URL <https://openreview.net/forum?id=FXWwYzlp8a>.
- Hendrycks, D., Burns, C., Kadavath, S., Arora, A., Basart, S., Tang, E., Song, D., and Steinhardt, J. Measuring mathematical problem solving with the math dataset. *NeurIPS*, 2021.
- Hui, B., Yang, J., Cui, Z., Yang, J., Liu, D., Zhang, L., Liu, T., Zhang, J., Yu, B., Dang, K., et al. Qwen2. 5-coder technical report. *arXiv preprint arXiv:2409.12186*, 2024.
- Li, H., Basri, R., and Kluger, Y. Likelihood training of cascaded diffusion models via hierarchical volume-preserving maps. In *The Twelfth International Conference on Learning Representations*, 2024. URL <https://openreview.net/forum?id=sojpn00o8z>.
- Li, T., Chen, M., Guo, B., and Shen, Z. A survey on diffusion language models, 2025. URL <https://arxiv.org/abs/2508.10875>.
- Lipman, Y., Chen, R. T. Q., Ben-Hamu, H., Nickel, M., and Le, M. Flow matching for generative modeling. In *The Eleventh International Conference on Learning Representations*, 2023. URL <https://openreview.net/forum?id=PqvMRDCJT9t>.
- Liu, J., Xia, C. S., Wang, Y., and Zhang, L. Is your code generated by chatGPT really correct? rigorous evaluation of large language models for code generation. In *Thirty-seventh Conference on Neural Information Processing Systems*, 2023a. URL <https://openreview.net/forum?id=1qvx610Cu7>.
- Liu, J., Liu, G., Liang, J., Li, Y., Liu, J., Wang, X., Wan, P., ZHANG, D., and Ouyang, W. Flow-GRPO: Training flow matching models via online RL. In *The Thirty-ninth Annual Conference on Neural Information Processing Systems*, 2025. URL <https://openreview.net/forum?id=oCBKGw5HNf>.
- Liu, X., Gong, C., and qiang liu. Flow straight and fast: Learning to generate and transfer data with rectified flow. In *The Eleventh International Conference on Learning Representations*, 2023b. URL <https://openreview.net/forum?id=XVjTT1nw5z>.
- Lou, A., Meng, C., and Ermon, S. Discrete diffusion modeling by estimating the ratios of the data distribution. In *Proceedings of the 41st International Conference on Machine Learning, ICML'24. JMLR.org*, 2024.
- Ni, J., Liu, Q., Du, C., Dou, L., Yan, H., Wang, Z., Pang, T., and Shieh, M. Q. Training optimal large diffusion language models, 2025. URL <https://arxiv.org/abs/2510.03280>.
- Nie, S., Zhu, F., You, Z., Zhang, X., Ou, J., Hu, J., ZHOU, J., Lin, Y., Wen, J.-R., and Li, C. Large language diffusion models. In *The Thirty-ninth Annual Conference on Neural Information Processing Systems*, 2025. URL <https://openreview.net/forum?id=KnqiC0znVF>.
- Onken, D., Fung, S. W., Li, X., and Ruthotto, L. Ot-flow: Fast and accurate continuous normalizing flows via optimal transport, 2021. URL <https://arxiv.org/abs/2006.00104>.
- Rein, D., Hou, B. L., Stickland, A. C., Petty, J., Pang, R. Y., Dirani, J., Michael, J., and Bowman, S. R. GPQA: A graduate-level google-proof q&a benchmark. In *First Conference on Language Modeling*, 2024. URL <https://openreview.net/forum?id=Ti67584b98>.
- Sakaguchi, K., Bras, R. L., Bhagavatula, C., and Choi, Y. Winogrande: An adversarial winograd schema challenge at scale, 2019. URL <https://arxiv.org/abs/1907.10641>.
- Schulman, J., Levine, S., Moritz, P., Jordan, M. I., and Abbeel, P. Trust region policy optimization, 2017a. URL <https://arxiv.org/abs/1502.05477>.
- Schulman, J., Wolski, F., Dhariwal, P., Radford, A., and Klimov, O. Proximal policy optimization algorithms, 2017b. URL <https://arxiv.org/abs/1707.06347>.
- Shao, Z., Wang, P., Zhu, Q., Xu, R., Song, J., Bi, X., Zhang, H., Zhang, M., Li, Y. K., Wu, Y., and Guo, D. Deepseekmath: Pushing the limits of mathematical reasoning in open language models, 2024. URL <https://arxiv.org/abs/2402.03300>.

- Song, Y., Sohl-Dickstein, J., Kingma, D. P., Kumar, A., Ermon, S., and Poole, B. Score-based generative modeling through stochastic differential equations, 2021. URL <https://arxiv.org/abs/2011.13456>.
- Tian, K., Jiang, Y., Yuan, Z., PENG, B., and Wang, L. Visual autoregressive modeling: Scalable image generation via next-scale prediction. In *The Thirty-eighth Annual Conference on Neural Information Processing Systems*, 2024. URL <https://openreview.net/forum?id=gojL67CfS8>.
- Tuo, P., Zeng, Z., Chen, J., and Cheng, B. Scalable multitemperature free energy sampling of classical ising spin states, 2025. URL <https://arxiv.org/abs/2503.08063>.
- Wang, C., Rashidinejad, P., Su, D., Jiang, S., Wang, S., Zhao, S., Zhou, C., Shen, S. Z., Chen, F., Jaakkola, T., Tian, Y., and Liu, B. Spg: Sandwiched policy gradient for masked diffusion language models, 2025a. URL <https://arxiv.org/abs/2510.09541>.
- Wang, X., Xu, C., Jin, Y., Jin, J., Zhang, H., and Deng, Z. Diffusion llms can do faster-than-ar inference via discrete diffusion forcing, 2025b. URL <https://arxiv.org/abs/2508.09192>.
- Wang, Y., Yang, L., Li, B., Tian, Y., Shen, K., and Wang, M. Revolutionizing reinforcement learning framework for diffusion large language models, 2025c. URL <https://arxiv.org/abs/2509.06949>.
- Wei, C., Yu, J., He, Y. T., Dong, H., Shu, Y., and Yu, F. Redit: Reward dithering for improved LLM policy optimization. In *The Thirty-ninth Annual Conference on Neural Information Processing Systems*, 2025. URL <https://openreview.net/forum?id=pG1Y63MqHm>.
- Wu, C., Zhang, H., Xue, S., Liu, Z., Diao, S., Zhu, L., Luo, P., Han, S., and Xie, E. Fast-dllm: Training-free acceleration of diffusion llm by enabling kv cache and parallel decoding, 2025. URL <https://arxiv.org/abs/2505.22618>.
- Xiong, L., Wang, H., Chen, X., Sheng, L., Xiong, Y., Liu, J., Xiao, Y., Chen, H., Han, Q.-L., and Tang, Y. Deepseek: Paradigm shifts and technical evolution in large ai models, 2025. URL <https://arxiv.org/abs/2507.09955>.
- Yang, L., Tian, Y., Li, B., Zhang, X., Shen, K., Tong, Y., and Wang, M. MMaDA: Multimodal large diffusion language models. In *The Thirty-ninth Annual Conference on Neural Information Processing Systems*, 2025. URL <https://openreview.net/forum?id=wczmXLuLGD>.
- Ye, J., Gao, J., Gong, S., Zheng, L., Jiang, X., Li, Z., and Kong, L. Beyond autoregression: Discrete diffusion for complex reasoning and planning. In *The Thirteenth International Conference on Learning Representations*, 2025a. URL <https://openreview.net/forum?id=NRYgUzSPZz>.
- Ye, J., Xie, Z., Zheng, L., Gao, J., Wu, Z., Jiang, X., Li, Z., and Kong, L. Dream 7b: Diffusion large language models. *arXiv preprint arXiv:2508.15487*, 2025b.
- Yu, R., Li, Q., and Wang, X. Discrete diffusion in large language and multimodal models: A survey, 2025. URL <https://arxiv.org/abs/2506.13759>.
- Zellers, R., Holtzman, A., Bisk, Y., Farhadi, A., and Choi, Y. Hellaswag: Can a machine really finish your sentence?, 2019. URL <https://arxiv.org/abs/1905.07830>.
- Zeng, H., Jiang, D., Wang, H., Nie, P., Chen, X., and Chen, W. ACECODER: Acing coder RL via automated test-case synthesis. In Che, W., Nabende, J., Shutova, E., and Pilehvar, M. T. (eds.), *Proceedings of the 63rd Annual Meeting of the Association for Computational Linguistics (Volume 1: Long Papers)*, pp. 12023–12040, Vienna, Austria, July 2025. Association for Computational Linguistics. ISBN 979-8-89176-251-0. doi: 10.18653/v1/2025.acl-long.587. URL <https://aclanthology.org/2025.acl-long.587/>.
- Zhan, A. Principled and tractable rl for reasoning with diffusion language models, 2025. URL <https://arxiv.org/abs/2510.04019>.
- Zhang, J., Hao, Z., Xia, W., Dong, H., Wang, H., Wei, C., Zhou, Y., Qi, Y., Lin, Q., and Cao, J. Gapo: Robust advantage estimation for real-world code llms, 2026. URL <https://arxiv.org/abs/2510.21830>.
- Zhang, Y., Gu, J., Wu, Z., Zhai, S., Susskind, J. M., and Jaitly, N. PLANNER: Generating diversified paragraph via latent language diffusion model. In *Thirty-seventh Conference on Neural Information Processing Systems*, 2023. URL <https://openreview.net/forum?id=SLWg8UUVS8Y>.
- Zhao, S., Gupta, D., Zheng, Q., and Grover, A. d1: Scaling reasoning in diffusion large language models via reinforcement learning. In *The Thirty-ninth Annual Conference on Neural Information Processing Systems*, 2025. URL <https://openreview.net/forum?id=7ZVR1BFuEv>.
- Zheng, C., Liu, S., Li, M., Chen, X.-H., Yu, B., Gao, C., Dang, K., Liu, Y., Men, R., Yang, A., Zhou, J., and Lin, J. Group sequence policy optimization, 2025a. URL <https://arxiv.org/abs/2507.18071>.

Zheng, K., Chen, H., Ye, H., Wang, H., Zhang, Q., Jiang, K., Su, H., Ermon, S., Zhu, J., and Liu, M.-Y. Diffusionft: Online diffusion reinforcement with forward process, 2025b. URL <https://arxiv.org/abs/2509.16117>.

Zhu, F., Wang, R., Nie, S., Zhang, X., Wu, C., Hu, J., Zhou, J., Chen, J., Lin, Y., Wen, J.-R., and Li, C. Llada 1.5: Variance-reduced preference optimization for large language diffusion models, 2025. URL <https://arxiv.org/abs/2505.19223>.

Zhuo, T. Y., Chien, V. M., Chim, J., Hu, H., Yu, W., Widyasari, R., Yusuf, I. N. B., Zhan, H., He, J., Paul, I., Brunner, S., GONG, C., Hoang, J., Zebaze, A. R., Hong, X., Li, W.-D., Kaddour, J., Xu, M., Zhang, Z., Yadav, P., Jain, N., Gu, A., Cheng, Z., Liu, J., Liu, Q., Wang, Z., Lo, D., Hui, B., Muennighoff, N., Fried, D., Du, X., de Vries, H., and Werra, L. V. Bigcodebench: Benchmarking code generation with diverse function calls and complex instructions. In *The Thirteenth International Conference on Learning Representations*, 2025. URL <https://openreview.net/forum?id=YrycTjlllL0>.

A. Detailed Derivation of the Cross-Entropy Gradient

In this section, we provide a step-by-step derivation of the gradient of the Cross-Entropy loss with respect to the pre-softmax logits. This derivation formally proves that the optimization direction of standard dLLM training is mathematically identical to the residual error vector in FM.

A.1. Definitions and Notation

Let the vocabulary size be V . We define the following variables:

- $\mathbf{z} \in \mathbb{R}^V$: The vector of pre-softmax logits output by the model, where z_i is the logit for the i -th token.
- $\mathbf{p} \in \Delta^{V-1}$: The probability distribution obtained by applying the Softmax function to \mathbf{z} :

$$p_k = \text{Softmax}(\mathbf{z})_k = \frac{e^{z_k}}{\sum_{j=1}^V e^{z_j}}. \quad (13)$$

- $\mathbf{y} \in \{0, 1\}^V$: The one-hot ground truth vector, where $y_c = 1$ for the correct class c , and $\sum_{j=1}^V y_j = 1$.
- \mathcal{L} : The Cross-Entropy loss for a single sample:

$$\mathcal{L} = - \sum_{j=1}^V y_j \log(p_j). \quad (14)$$

Our goal is to compute the gradient $\frac{\partial \mathcal{L}}{\partial z_i}$ for an arbitrary logit z_i .

A.2. Step 1: Derivative of the Softmax Function

First, we compute the partial derivative of the softmax output p_j with respect to the logit z_i . Using the quotient rule, we distinguish between two cases:

Case 1: $i = j$

$$\frac{\partial p_i}{\partial z_i} = \frac{e^{z_i}(\sum e^{z_k}) - e^{z_i}e^{z_i}}{(\sum e^{z_k})^2} = \frac{e^{z_i}}{\sum e^{z_k}} \left(1 - \frac{e^{z_i}}{\sum e^{z_k}}\right) = p_i(1 - p_i). \quad (15)$$

Case 2: $i \neq j$

$$\frac{\partial p_j}{\partial z_i} = \frac{0 - e^{z_j}e^{z_i}}{(\sum e^{z_k})^2} = -\frac{e^{z_j}}{\sum e^{z_k}} \frac{e^{z_i}}{\sum e^{z_k}} = -p_j p_i. \quad (16)$$

Using the Kronecker delta δ_{ij} (where $\delta_{ij} = 1$ if $i = j$, else 0), we can unify these expressions:

$$\frac{\partial p_j}{\partial z_i} = p_j(\delta_{ij} - p_i). \quad (17)$$

A.3. Step 2: Applying the Chain Rule

We apply the chain rule to finding the gradient of the loss \mathcal{L} with respect to z_i . Since \mathcal{L} depends on all p_j , we sum over all j :

$$\frac{\partial \mathcal{L}}{\partial z_i} = \sum_{j=1}^V \frac{\partial \mathcal{L}}{\partial p_j} \cdot \frac{\partial p_j}{\partial z_i}. \quad (18)$$

First, the derivative of the Cross-Entropy loss with respect to p_j is:

$$\frac{\partial \mathcal{L}}{\partial p_j} = \frac{\partial}{\partial p_j} \left(- \sum_{k=1}^V y_k \log(p_k) \right) = -\frac{y_j}{p_j}. \quad (19)$$

Substituting this and Eq. (17) into the chain rule equation:

$$\begin{aligned}
 \frac{\partial \mathcal{L}}{\partial z_i} &= \sum_{j=1}^V \left(-\frac{y_j}{p_j} \right) \cdot p_j (\delta_{ij} - p_i) \\
 &= - \sum_{j=1}^V y_j (\delta_{ij} - p_i) \\
 &= - \left(\sum_{j=1}^V y_j \delta_{ij} - \sum_{j=1}^V y_j p_i \right).
 \end{aligned} \tag{20}$$

We analyze the two terms in the summation:

1. The first term $\sum_{j=1}^V y_j \delta_{ij}$ is non-zero only when $j = i$, so it simplifies to y_i .
2. The second term $\sum_{j=1}^V y_j p_i$ allows us to factor out p_i since it does not depend on j . Since \mathbf{y} is a one-hot vector (or valid probability distribution), $\sum_{j=1}^V y_j = 1$. Thus, the term simplifies to $p_i \cdot 1 = p_i$.

Substituting these back, we obtain:

$$\frac{\partial \mathcal{L}}{\partial z_i} = -(y_i - p_i) = p_i - y_i. \tag{21}$$

A.4. Conclusion: Vector Field Interpretation

Expressing the result in vector notation, the gradient of the Cross-Entropy loss is:

$$\nabla_{\mathbf{z}} \mathcal{L}_{CE} = \mathbf{p} - \mathbf{y}. \tag{22}$$

Recall from our definition in Section 3 that the model velocity field is $v_\theta = \mathbf{p} - \mathbf{m}$ and the target velocity field is $u_t = \mathbf{y} - \mathbf{m}$. The error vector in FM is:

$$v_\theta - u_t = (\mathbf{p} - \mathbf{m}) - (\mathbf{y} - \mathbf{m}) = \mathbf{p} - \mathbf{y}. \tag{23}$$

Final Result: Since $\nabla_{\mathbf{z}} \mathcal{L}_{CE} = v_\theta - u_t$, minimizing the Cross-Entropy loss is dynamically equivalent to minimizing the velocity error in FM. This confirms the theoretical isomorphism: dLLMs are implicitly trained to match the discrete velocity field on the simplex.